AIP | Applied Physics Letters

Integrated sensor for ultra-thin layer sensing based on hybrid coupler with short-range surface plasmon polariton and dielectric waveguide

Boyu Fan, Fang Liu, Xiaoyan Wang, Yunxiang Li, Kaiyu Cui et al.

Citation: Appl. Phys. Lett. **102**, 061109 (2013); doi: 10.1063/1.4792319
View online: http://dx.doi.org/10.1063/1.4792319
View Table of Contents: http://apl.aip.org/resource/1/APPLAB/v102/i6
Published by the American Institute of Physics.

Integrated sensor for ultra-thin layer sensing based on hybrid coupler with short-range surface plasmon polariton and dielectric waveguide

Boyu Fan, Fang Liu, Xiaoyan Wang, Yunxiang Li, Kaiyu Cui, Xue Feng, and Yidong Huang
State Key Lab of Integrated Optoelectronics, Department of Electronic Engineering, Tsinghua University, Beijing 100084, China

(Received 17 August 2012; accepted 1 February 2013; published online 13 February 2013)

Based on a hybrid coupler composed of short-range surface plasmon polariton (SRSPP) and dielectric waveguides, an integrated sensor for ultra-thin layer sensing has been realized. The simulation and experiment results demonstrate that the thickness variation of detection layer (polymer layer) about several nanometers could be detected. The measured thickness-detection sensitivity is as high as 0.67 dB/nm. And the sensitive region for thickness variation of polymer layer can be adjusted widely by varying the thickness of the SRSPP waveguide. © *2013 American Institute of Physics*. [http://dx.doi.org/10.1063/1.4792319]

A surface plasmon polariton (SPP) is a transverse-magnetic surface electromagnetic excitation that propagates along an interface between a metal and a dielectric medium.[1] The significant response of SPP to a variation in external refractive index plays a critical role in chemical and biological sensing technology.[2–10] As is well known, the detection of small molecules with size only in the range from several to hundreds of nanometers, such as He,[3] bisphenol A,[4] proteins,[5] and benzo[a]pyrene,[8,9] has received more and more extensive attention in various application of disease diagnosis, food security, environment monitoring, and so on. For these applications, real-time and field test is an important issue. Therefore, the integration of sensor with rather small size and low cost has to be considered. Up to now, various integrated SPP sensors have been reported with different metallic nanostructures, such as metal strips waveguides,[10] fiber-optic waveguide structure,[11] metal–insulator–metal waveguides,[12,13] photonic crystal waveguide,[14] and so on. However, the sensitivity of the integrated SPP sensor worsens significantly when reducing the thickness of detection layer to tens of nanometers, which is rather thin compared with the field size of conventional SPP mode. Moreover, utilizing the spectrometer as the output signal detector is not suitable for the integration of the sensing system and real-time and field test.

The short-range SPP (SRSPP) mode is a type of SPP mode guided by a thin metal film with a field highly bounded on the surface of the metal film, which is promising for ultra-thin layer detection,[6] because its mode size is only a fraction of the incidence wavelength.[2] Recently, our group has proposed a vertical SPP-dielectric coupler. Based on this structure, long-range SPP (LRSPP) and SRSPP have been excited efficiently using an integratable approach,[15–17] and it is demonstrated theoretically and experimentally that the coupling between the SPP mode and the dielectric waveguide (DW) mode is very sensitive to the refractive index of analytes on the metal surface. As a result, by monitoring the output power of the dielectric waveguide, this hybrid coupler has great potential for realizing an integrated biological and chemical sensor with rather high sensitivity.[15,18,19] Based on our previous works, where the thick detection layer was studied, in this paper, the ultrathin layer sensing characteristics of the integrated sensor have been studied theoretically and experimentally. The simulation results indicate that, because the highly bounded field of SRSPP could effectively feel the change of ultra-thin layer variation, the output power of the sensor is rather sensitive to the variation of the thickness of detection layer h_{det} even though h_{det} is only dozens of nanometers. For h_{det} changing 1 nm, variation of 1.65 dB in output power can be obtained. Subsequently, the integrated sensors with different parameters are fabricated, and the nanometer-thick polyelectrolyte layer with controllable thickness and refractive index is prepared above the metal film by utilizing the self-assembly method.[20] The measurement results are in good agreement with the theoretical results, where the output power is very sensitive to the thickness of the detection layer h_{det} because the variation of the thickness changes the effective index. Even 5 nm-thick variation of molecular layer can be detected. Since the detection signal is output power in our proposed sensor, comparing to that utilizing spectrograph as the output signal detector,[3–14] the hybrid coupler sensor is essentially propitious to integration. Furthermore, it has been observed that the sensitive region of h_{det}, around which output power varies significantly, can be adjusted by varying the thickness of the metal film, which makes the sensing application flexible.

Figure 1 shows the schematic structure of the integrated sensor, which is based on a hybrid coupler composed of a SRSPP waveguide and a DW. Surrounding the two waveguides is the dielectrics SiO_2 with refractive index n_s. The sensing region with length L along the z-direction is located on the SRSPP waveguide (Au strip). The sectional view of the hybrid coupler sensor in the x–y plane and the detailed structure parameters are presented in Fig. 1(b).

For the integrated sensor shown in Fig. 1, the previous search results indicate that the energy coupling efficiency between the SiN_x waveguide and SPP waveguide, as well as the output power of the SiN_x waveguide, is rather sensitive to the refractive index of substance on the metal surface.[18,19] Changing the thickness of the detection layer is actually varying the refractive index of the detection layer and could affect the output power of the sensor. Nevertheless, if it is

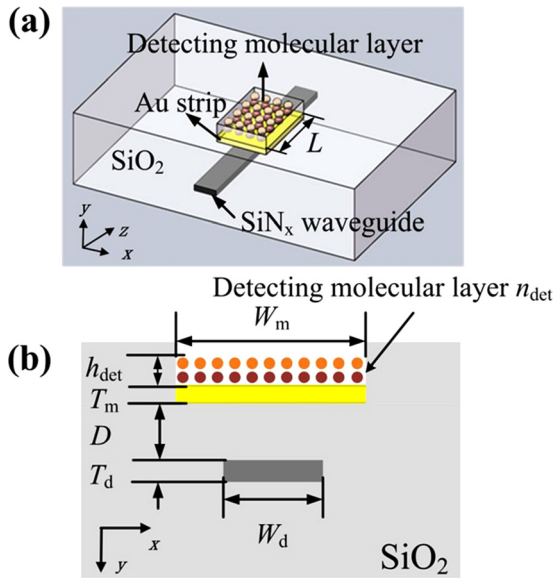

FIG. 1. (a) Schematic structure of the integrated sensor based on the SRSPP-SiN_x vertical coupler with Au strip (yellow) and SiN_x strip (gray) embedded in SiO_2. (b) Sectional view of the sensor in the x-y plane (Au strip with thickness $T_m = 17$ nm, width $W_m = 8\,\mu$m, and dielectric constant $\varepsilon_m = -132 + i \times 12.65$;[21] SiN_x strip with thickness $T_d = 175$ nm, width $W_d = 3\,\mu$m, and refractive index $n_d = 2$;[21] Distance between the two waveguides $D = 1.5\,\mu$m; refractive index of surrounding material SiO_2 $n_s = 1.444$ (Ref. 21)).

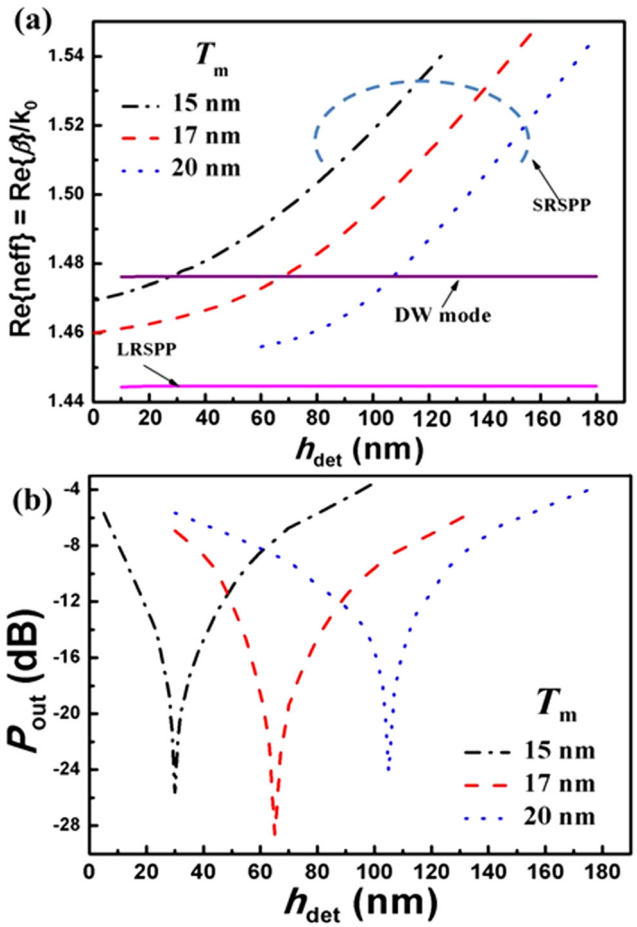

FIG. 2. (a) Relative propagation constant Re{n_{eff}} of SRSPP labeled with different thicknesses of the metal film and LRSPP mode of individual Au waveguide as a function of h_{det}. The purple line corresponds to Re{n_{eff}} of the dielectric waveguide supported by SiN_x waveguide. (b) Output power P_{out} as a function of h_{det} when n_{det} is setting to 1.495 labeled with different thicknesses of the metal film.

expected to get the obvious output power change, two conditions should be met. First, the relative propagation constant of individual SRSPP (Re{n_{eff}}) and SiN_x waveguide mode should be close to each other when changing the thickness or refractive index of the detection layer.[15,16] Second, the thickness change occurring in the region of mode field should be comparable with the size of the SPP mode. Based on this concept, the parameters of the sensor are designed and the ultra-thin layer sensing characteristics are studied by finite element method and modal-expansion method.[22] The detailed simulation method is similar to that described in Ref. 19, with the only difference being that the thickness of detection layer is decreased to dozens of nanometers and the refractive index of detection layer is set to be 1.495, considering the refractive index of the polymer layer to be detected in the experiment.[20] Above the detection layer, there is infinite thick water layer (refractive index $n = 1.333$). The other structure parameters for simulation are listed in the caption of Fig. 1.

Figure 2(a) shows that the relative propagation constant (Re{n_{eff}}) of DW mode and the SRSPP mode as a function of h_{det}. For $T_m = 15$ nm, the Re{n_{eff}} of SRSPP and DW mode matches well at the crossing point of $h_{det} = 30$ nm. In this case, most of the power couples from DW mode to SPP mode when the sensing length $L \approx m \times L_c$ (coupling length $L_c = \pi/(\beta_{Ar}\text{-}\beta_{Br})$, β_{Ar} and β_{Br} are the real part of complex propagation constants of the two coupled eigenmodes supported by the hybrid coupler, $m = 1, 3, 5, 7, \ldots$).[18] Thus, at the optimized length $L = 106\,\mu$m, the output power of DW mode P_{out} reaches the minimum value corresponding to the dip of the black curve shown in Fig. 2(b). When the h_{det} deviates from 30 nm, the Re{n_{eff}} of the individual SRSPP mode deviates from that of the SiN_x waveguide mode, and the coupling between the two waveguides mode becomes weak, which results in the larger output power from the SiN_x waveguide. To be noticed, in the range of $h_{det} = 30$–35 nm, the change of the output power is 8.26 dB. Here, defining the thickness-detection sensitivity (TDS) as $\Delta P_{out}/\Delta h_{det}$, the average TDS is approximately 1.65 dB/nm, which indicates a rather high sensitivity for ultra-thin layer detection. Compared to conventional thickness detection sensor,[23,24] our proposed hybrid coupler sensor with output power as detection signal is propitious to integration and has higher sensitivity for ultra-thin layer detection. In addition, with increasing the Au thickness T_m, the Re{n_{eff}} crossing points of the two waveguides mode shown in Fig. 2(a) move to larger h_{det}. Thus, the corresponding sensing curves illustrated in Fig. 2(b) get the minimum P_{out} when $h_{det} = 65$ nm and 105 nm, respectively. By the way, owing to the much more diffuse mode field of LRSPP compared with SRSPP mode, LRSPP cannot effectively feel the change of ultra-thin layer variation, which is revealed by the straight pink line in Fig. 2(b).

To verify the simulation results, the integrated sensor based on the SRSPP-dielectric hybrid coupler sensor is fabricated, and the detailed fabrication processes are similar to that depicted in Ref. 19. Moreover, the sensors with Au strip of different lengths and thicknesses ($L = 80$–150 μm, with an

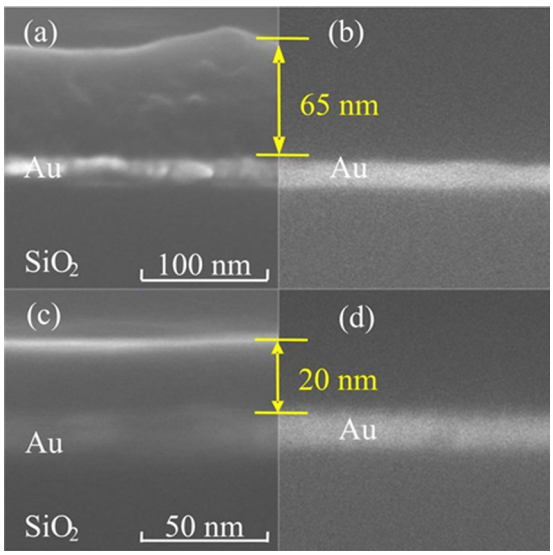

FIG. 3. The SEM photo of polymer multilayer grown on the gold surface. (a) and (c) secondary electron imaging; (b) and (d) back-scattered electrons imaging.

interval of 10 μm; $T_m = 15$ nm, 17 nm, and 20 nm) are fabricated. Subsequently, the self-assembly method is adopted to obtain the ultrathin detection layer with polyelectrolytes purchased from Aldrich without further purification,[20] including poly(sodium 4-styrenesulfonate) (PSS, MW = 70 000), cationic poly(allylamine hydrochloride) (PAH, MW = 65 000), and cationic poly(ethyleneimine) (PEI, MW = 70 000). Sodium chloride (purity > 99.5%) is purchased from Fluka, and its 0.9 M solution is used as dissolvent for these polyelectrolytes and buffer/rinse solution in the experiment. First, the SRSPP-coupling sensor is immersed into 100 μl of 0.9 M NaCl solution and incubated for 5 min to establish a stability baseline. 5 μl PEI solution is substituted for NaCl solution and allowed to incubate for 5 min. Subsequently, the sensor chip is rinsed and monitored with buffer for 5 min. PSS and PAH are alternately absorbed on the PEI surface using the same procedure as PEI. In addition, a buffer rinse is used after every PSS and PAH incubation to re-establish a baseline. Progressively, a ultrathin PEI-(PSS-PAH)$_n$ detection layer is deposited on the sensor surface. In view of the fact that the growth of each layer in the multilayer stack is self-limiting, the thickness of each layer is about 5 nm.[20] Figure 3 shows the SEM images of polyelectrolyte multilayer prepared above the gold film with 13 layers (Figs. 3(a) and 3(b)) and 4 layers (Figs. 3(c) and 3(d)), respectively.

Here, the chip is cut into 2.5-mm-long pieces for easier measurement. In the fiber-to-waveguide butt-coupling measurement,[17,19] the output power of the sensor is recorded once a layer of polyelectrolyte is deposited on the chip. Considering the optimized sensing length in the simulation results is 106 μm, the sensing characteristics of the hybrid coupler sensor with $L = 90$, 100, and 110 μm are measured. It is found that the sensor with $L = 100$ μm has the best performance. Figure 4 shows the measured output power P_{TM}/P_{TE} (dB) from the SiN_x waveguide versus the thickness of detection layer h_{det}. For the sensor with $T_m = 15$ nm, the output power varies significantly as a function of the thickness of polyelectrolyte layer h_{det} and the minimum P_{out} is obtained when $h_{det} = 25$ nm. By the way, each point is derived by measuring three samples with the same structure parameters, and the small deviation of every point in the three curves indicates that the sensors have good consistency in sensing performance.

Figure 4(b) shows that the output power P_{TM}/P_{TE} changes with the thickness of detection layer when $T_m = 17$ nm. In this case, owing to the shift of relative propagation constant Re{n_{eff}} introduced by the variation of metal film thickness as shown in Fig. 2(b), the minimum P_{out} moves to about 55 nm compared with Fig. 4(a) and the average TDS is as high as 0.67 dB/nm in the range of 50–55 nm. Subsequently, when the thickness of metal film T_m is further increased to 20 nm, the dip of the curve shifting to $h_{det} = 90$ nm is observed owing to the variation of the propagation constant of SRSPP mode. Therefore, it is verified that SRSPP-dielectric hybrid coupler sensor can be applied for ultrathin sensing, such as small bio- or chemical molecules detection.

Compared with the simulation results shown in Fig. 2(b), the output power contrast (the largest change of P_{out}) is much smaller indicating the relatively lower sensitivity. This may be ascribed to two reasons: First, the fabrication error results in the deviation of L in the experiment from the optimal value; second, the thickness variation of detection layer in the experiment (5 nm) is much larger than that in the simulation (0.5 nm), which influences the P_{out} to reach a rather low value. Thus, by optimizing the sensing length L and monitoring the constant thickness variation of detection

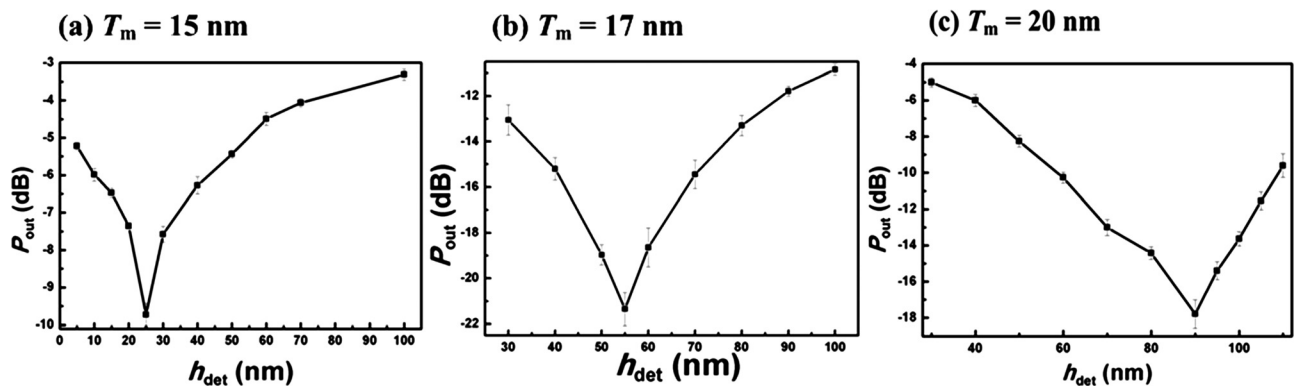

FIG. 4. The measured output P_{TM}/P_{TE} ratio (black triangles with error-bar) versus the thickness of the detection layer h_{det} labeled with different Au thicknesses, (a) $T_m = 15$ nm, (b) $T_m = 17$ nm, and (c) $T_m = 20$ nm.

layer, rather high output power contrast similar to the simulation results should be derived.

In conclusion, the ultrathin layer sensing characteristics of an integrated sensor based on a vertical SRSPP-dielectric hybrid coupler sensor have been studied theoretically and experimentally. The simulation results show that the output power changes significantly with nanometer-thick variation of the detection layer due to the highly bounded field of SRSPP. By preparing a polymer layer with controllable thickness and refractive index on the surface of the sensor with self-assembly method, it is observed that even 5 nm-thick variation of molecular layer is easy to be detected with sensitivity ($\Delta P_{out}/\Delta h_{det}$) as high as 0.67 dB/nm, which would have rather high sensitivity for small bio-chem molecule detection and be conducive to the integration. In addition, the sensitive region of h_{det} can be adjusted widely by varying the thickness of the SRSPP waveguide.

This work was supported by the National Basic Research Programs of China (973 Program) under Contract Nos. 2011CB301803, 2010CB327405, and 2011CBA00608, and by the National Natural Science Foundation of China (NSFC-61036011, 61107050, and 61036010). The authors thank Professor Jiangde Peng, Professor Wei Zhang, Dr. Xue Feng, and Kaiyu Cui, as well as Mr. H. Takatsu and A. Kamisawa of the ROHM Corporation, for their helpful comments.

[1]J. J. Bruke and G. I. Stegeman, Phys. Rev. B **33**, 5186 (1986).
[2]J. Homola, S. S. Yee, and G. Gauglitz, Sens. Actuators B **54**, 3 (1999).
[3]J. M. Bingham, J. N. Anker, L. E. Kreno, and R. P. Van Duyne, J. Am. Chem. Soc. **132**, 17358 (2010).
[4]K. Hegnerová and J. Homola, Sens. Actuators B **151**, 177 (2010).
[5]O. Salihoglu, S. Balci, and C. Kocabas, Appl. Phys. Lett. **100**, 213110 (2012).
[6]J. Guo, P. D. Keathley, and J. T. Hastings, Opt. Lett. **33**, 512 (2008).
[7]A. V. Whitney, J. W. Elam, S. L. Zou, A. V. Zinovev, P. C. Stair, G. C. Schatz, and R. P. Van Duyne, J. Phys. Chem. B **109**, 20522 (2005).
[8]J. Dostálek, J. Přibyl, J. Homola, and P. Skládal, Anal. Bioanal. Chem. **389**, 1841 (2007).
[9]S. Boujday, C. Gu, M. Girardot, M. Salmain, and C. Pradier, Talanta **78**, 165 (2009).
[10]Y. H. Joo, S. H. Song, and R. Magnusson, Appl. Phys. Lett. **97**, 201105 (2010).
[11]J. H. Ahn, T. Y. Seong, W. M. Kim, T. S. Lee, I. Kim, and K. S. Lee, Opt. Express **20**, 21729 (2012).
[12]M. Tamura and H. Kagata, IEEE Trans. Microw. Theory Tech. **58**, 3954–3960 (2010).
[13]D. J. Lee, H. D. Yim, S. G. Lee, and B. H. O, Opt. Express **19**, 19895 (2011).
[14]T. Srivastava, R. Das, and R. Jha, Plasmonics **7**, 1557–1955 (2012).
[15]F. Liu, R. Wan, Y. Huang, and J. Peng, Opt. Lett. **34**, 2697 (2009).
[16]R. Wan, F. Liu, X. Tang, Y. Huang, and J. Peng, Appl. Phys. Lett. **94**, 141104 (2009).
[17]R. Wan, F. Liu, Y. Huang, B. Fan,Y. Miura, D. Ohnishi, Y. Li, H. Li, and Y. Xia, Appl. Phys. Lett. **97**, 141105 (2010).
[18]R. Wan, F. Liu, and Y. Huang, Opt. Lett. **35**, 244 (2010).
[19]B. Fan, F. Liu, Y. Li, Y. Huang, Y. Miura, and D. Ohnishi, Appl. Phys. Lett. **100**, 111108 (2012).
[20]B. Cunningham, B. Lin, J. Qiu, P. Li, J. Pepper, and B. Hugh, Sens. Actuators B **85**, 219 (2002).
[21]E. D. Palik, *Handbook of Optical Constants of Solids* (Academic, Orlando, FL, 1985).
[22]H. S. Won, K. C. Kim, S. H. Song *et al.*, Appl. Phys. Lett. **88**, 011110 (2006).
[23]S. Wu, P. Guo, W. Huang, S. Xiao, and Y. Zhu, J. Phys. Chem. C **115**, 15205 (2011).
[24]M. Theuer, R. Beigang, and D. Grischkowsky, Appl. Phys. Lett. **97**, 071106 (2010).